AIP | The Journal of Chemical Physics

Two-photon absorption cross sections within equation-of-motion coupled-cluster formalism using resolution-of-the-identity and Cholesky decomposition representations: Theory, implementation, and benchmarks

Kaushik D. Nanda and Anna I. Krylov

Citation: The Journal of Chemical Physics **142**, 064118 (2015); doi: 10.1063/1.4907715
View online: http://dx.doi.org/10.1063/1.4907715
View Table of Contents: http://scitation.aip.org/content/aip/journal/jcp/142/6?ver=pdfcov
Published by the AIP Publishing

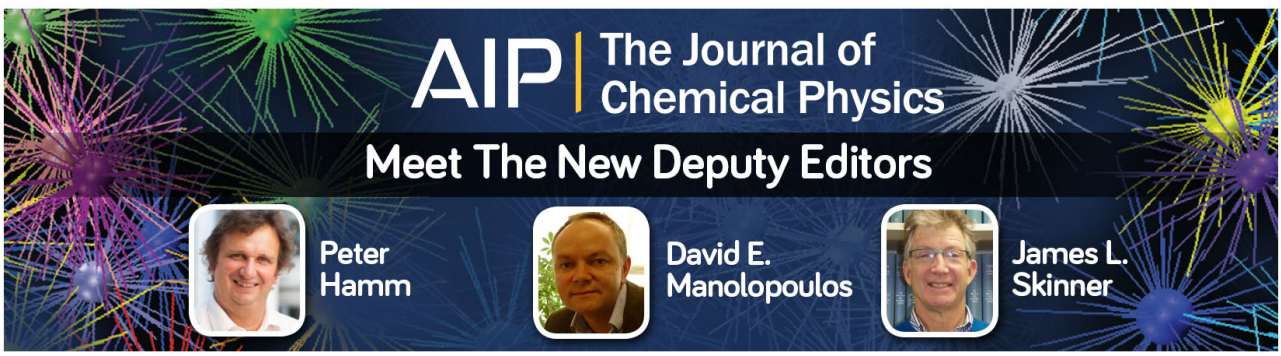

Two-photon absorption cross sections within equation-of-motion coupled-cluster formalism using resolution-of-the-identity and Cholesky decomposition representations: Theory, implementation, and benchmarks

Kaushik D. Nanda and Anna I. Krylov
Department of Chemistry, University of Southern California, Los Angeles, California 90089-0482, USA

(Received 12 December 2014; accepted 25 January 2015; published online 13 February 2015)

The equation-of-motion coupled-cluster (EOM-CC) methods provide a robust description of electronically excited states and their properties. Here, we present a formalism for two-photon absorption (2PA) cross sections for the equation-of-motion for excitation energies CC with single and double substitutions (EOM-CC for electronically excited states with single and double substitutions) wave functions. Rather than the response theory formulation, we employ the expectation-value approach which is commonly used within EOM-CC, configuration interaction, and algebraic diagrammatic construction frameworks. In addition to canonical implementation, we also exploit resolution-of-the-identity (RI) and Cholesky decomposition (CD) for the electron-repulsion integrals to reduce memory requirements and to increase parallel efficiency. The new methods are benchmarked against the CCSD and CC3 response theories for several small molecules. We found that the expectation-value 2PA cross sections are within 5% from the quadratic response CCSD values. The RI and CD approximations lead to small errors relative to the canonical implementation (less than 4%) while affording computational savings. RI/CD successfully address the well-known issue of large basis set requirements for 2PA cross sections calculations. The capabilities of the new code are illustrated by calculations of the 2PA cross sections for model chromophores of the photoactive yellow and green fluorescent proteins. [http://dx.doi.org/10.1063/1.4907715]

I. INTRODUCTION

Two-photon absorption (2PA) by a molecule in a single quantum act was first characterized theoretically, using perturbation theory, by Göppert-Mayer in 1931.[1] However, the first observations of this phenomenon were only realized three decades later, following the invention of lasers that are capable of delivering sufficiently high intensity.[2] 2PA is a non-linear optical process with a quadratic dependence of the absorption strength on the intensity of the incident light. Since two-photon transitions become allowed only in the second order of perturbation theory, 2PA cross sections are much smaller than the cross sections for one-photon absorption. As illustrated in Fig. 1, 2PA may entail a simultaneous absorption of two degenerate [Fig. 1(a)] or different energy [Fig. 1(b)] photons. If the energy of one of the photons matches the position of an intermediate electronic state [as in Fig. 1(c)], the cross sections may be significantly enhanced.

Owing to the quadratic dependence of the intensity, the 2P-based techniques offer better spatial resolution. Moreover, having two photons involved enables 3D spatial imaging. 2PA has been utilized in a variety of applications including drug delivery, photodynamic therapy, optical storage, high-resolution imaging, and fabrication of nanomachines.[3–18] These applications calling for materials with large 2PA cross sections have stimulated research aiming at understanding and quantifying 2PA phenomena, and at designing new materials with desired electronic properties.[19–21]

2PA spectroscopy is also very useful as a research tool. For example, by mapping out the polarization dependence of the 2PA cross section, it is possible to assign the symmetry of the excited-state wave function, even in isotropic liquids.[22–24] This continues to be a powerful technique in condensed-phase electronic spectroscopy, e.g., as recently as 2009, new information about the excited states of neat liquid water has been obtained from polarization-dependent 2PA.[25]

Experimental measurements of absolute 2PA cross sections are difficult due to competing optical processes such as stimulated emission and scattering that arise in high-intensity regime inherent in these experiments.[26] In biological systems such as photoactive proteins, there are additional calibration difficulties leading to significant discrepancies in the reported measurements of absolute 2PA cross sections.[27]

Computational methods capable of describing excited states and their properties (such as 2PA cross sections) can assist experimental studies, aid the interpretation of the results, and, ultimately, enable *in silico* design of new materials with desired non-linear optical properties. Numerous computational studies of 2PA phenomena have been reported in the past couple of decades. Owing to the low computational cost, most applications relied on time-dependent density functional theory (TDDFT).[19–21,28–33] However, known problems with the description of Rydberg and charge-transfer excited states may affect the accuracy of 2PA cross sections computed with DFT.[34] Therefore, it is desirable to use more reliable coupled-cluster (CC) methods, especially for calibration purposes. Until recently, CC methods were mostly used to compute 2PA cross sections in relatively small molecules.[34,35] 2PA cross sections computed with a lowest-level CC method,[36] CC2, have been reported for a large dye molecule, a molecular

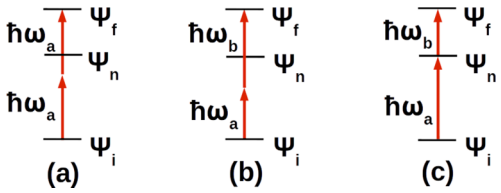

FIG. 1. Different types of resonant 2PA ($\omega_a + \omega_b = E_f - E_i$). Panels (a) and (b) depict 2PA with degenerate ($\omega_b = \omega_a$) and non-degenerate photons, respectively; panel (c) illustrates resonance-enhanced 2PA wherein the energy of one of the photons matches the position of an intermediate excited state.

tweezer complex,[37] and for chromophores of several photoactive proteins.[21,38]

As of today, CC implementations of 2PA cross sections are still scarce, owing to the additional complexity (relative to energy calculations) inherent for properties' calculations in quantum chemistry. The DALTON program[39] pioneered calculations of 2PA cross sections for the CC hierarchy of methods (CCS, CC2, CCSD, CC3) formulated within quadratic response theory.[34,35,40,41] This implementation enabled invaluable benchmark studies of the 2PA cross sections in small molecules.[34] The CC2-based 2PA calculations using resolution-of-the-identity (RI) approximations have been implemented[37] in Turbomole.[42] Recently, 2PA cross sections were implemented for the algebraic diagrammatic construction (ADC) method[43] within Q-Chem.[44]

We report the implementation of 2PA cross sections for the EOM-EE-CCSD (equation-of-motion for excitation energies CC with single and double substitutions) wave functions in the Q-Chem electronic structure program.[44,45]

Earlier formulations of 2PA cross sections for CC wave functions were based on the quadratic response theory.[41,46–50] A somewhat more direct approach utilizes the Lagrangian formalism in which response functions can be derived as derivatives of time-averaged quasienergy.[46–51] Here, we employ an alternative strategy for calculations of properties, the so-called expectation-value approach[52,53] in which one begins with the expression of a property derived for exact states and then uses approximate wave functions to evaluate the respective matrix elements. This strategy is commonly used for properties calculations within EOM-CC,[52,53] configuration interaction, and ADC approaches.[43]

In addition to the canonical implementation, we also exploit the intrinsic linear dependencies of the electronic repulsion integrals using their RI and Cholesky decomposition (CD) representations, significantly reducing the storage and I/O requirements in electronic structure calculations.[54–67] Our implementation of 2PA properties is based on the general implementation of the RI and CD representations of the four-index two-electron integrals within the framework of EOM-EE-CCSD that has been reported earlier.[68] For energy calculations, RI and CD EOM-CCSD implementations allow for significant speedups (of 85% and more, in particular, in large basis sets and when combined with frozen natural orbitals[69]) without compromising the accuracy.

As has been shown in earlier benchmark studies,[34] larger basis sets are needed for accurate predictions of 2PA cross sections than for energy calculations. In particular, in small molecules the converged results were only obtained when using doubly augmented Dunning's basis sets. While this might be an artifact of small molecules that have low-lying Rydberg states, it could be that even for large chromophores relatively large basis sets are needed for converged results. In light of this strong basis set dependence, RI/CD approximations become particularly attractive. As illustrated by our benchmarks, RI/CD approximations lead to small errors in 2PA cross sections relative to the canonical implementation (less than 4%), while significantly reducing storage and I/O requirements.

The structure of the paper is as follows. In Sec. II, we discuss the EOM-EE-CCSD method and how RI and CD representations of the two-electron integrals reduce I/O and storage bottlenecks. Then, we discuss the theory behind 2PA cross sections for exact states followed by the presentation of the expectation-value formulation for EOM-CCSD wave functions. Sections III–IV are dedicated to benchmarks and illustrative calculations of 2PA cross sections for chromophores of photoactive yellow protein (PYP) and green fluorescent protein (GFP); the results represent the highest-level calculations of 2PA cross sections for these chromophores. We also discuss the computational costs of the canonical, RI, and CD implementations.

II. THEORY

A. Equation-of-motion coupled-cluster method with single and double substitutions

The EOM-CC methods provide an efficient and robust computational approach for describing multiple electronic states including multi-configurational wave functions of electronically excited states.[53,70–75] The EOM-CC methods are similar, or equivalent (in some aspects), to linear response CC.[76–80] The EOM-CC wave function has the following form:

$$|\Psi\rangle = \hat{R}e^{\hat{T}}|\Phi_0\rangle, \tag{1}$$

where the linear EOM operator $\hat{R}$ acts on the reference CC wave function, $e^{\hat{T}}|\Phi_0\rangle$. The operator $\hat{T}$ is an excitation operator satisfying the reference-state CC equations

$$\langle\Phi_\mu|\bar{H}|\Phi_0\rangle = 0, \tag{2}$$

where Φ_μ are the μ-tuply excited (with respect to the reference determinant, Φ_0[81]) determinants, $\bar{H} = e^{-\hat{T}}\hat{H}e^{\hat{T}}$, and the reference CC energy is

$$\langle\Phi_0|\bar{H}|\Phi_0\rangle = E_{CC}. \tag{3}$$

The EOM amplitudes $\hat{R}$ and the corresponding energies are found by diagonalizing the similarity-transformed Hamiltonian, $\bar{H}$, in the space of target configurations defined by the choice of the operator $\hat{R}$ and the reference Φ_0 (see Ref. 73 for examples of different EOM models),

$$\bar{H}R^k = E_k R^k. \tag{4}$$

In EOM-CCSD, the CC and EOM operators are truncated as

$$\hat{T} = \hat{T}_1 + \hat{T}_2 \quad \text{and} \quad \hat{R} = R_0 + \hat{R}_1 + \hat{R}_2, \tag{5}$$

where only the single and double excitation operators ($1h1p$ and $2h2p$) are retained in $\hat{T}$ and $\hat{R}$ (in the case of EOM-EE),

$$\hat{T}_1 = \sum_{ia} t_i^a a^+ i; \quad \hat{T}_2 = \frac{1}{4} \sum_{ijab} t_{ij}^{ab} a^+ b^+ ji, \tag{6}$$

$$\hat{R}_1 = \sum_{ia} r_i^a a^+ i; \quad \hat{R}_2 = \frac{1}{4} \sum_{ijab} r_{ij}^{ab} a^+ b^+ ji. \tag{7}$$

Since $\bar{H}$ is a non-Hermitian operator, its left and right eigenstates, L^k and R^k, are not identical

$$\bar{H} R^k = E_k R^k, \tag{8}$$

$$L^k \bar{H} = L^k E_k, \tag{9}$$

$$\langle \Phi_0 L^m | R^n \Phi_0 \rangle = \delta_{mn}, \tag{10}$$

where $\hat{L} = \hat{L}_1 + \hat{L}_2 = \sum_{ia} l_i^a a^+ i + \frac{1}{4} \sum_{ijab} l_{ij}^{ab} a^+ b^+ ji$.

The expansion coefficients, l_i^a, l_{ij}^{ab}, r_i^a, and r_{ij}^{ab}, are found by diagonalizing $\bar{H}$. For energy calculations, only right eigenstates are needed; however for properties, both left and right eigenstates need to be computed.

In the basis of the reference, singly and doubly excited determinants, $\bar{H}$ assumes the following form:

$$\bar{H} = \begin{pmatrix} E_{CC} & \bar{H}_{0S} & \bar{H}_{0D} \\ 0 & \bar{H}_{SS} & \bar{H}_{SD} \\ 0 & \bar{H}_{DS} & \bar{H}_{DD} \end{pmatrix} \tag{11}$$

by virtue of CCSD Eqs. (2) and (3). Subtracting Eq. (3) from Eqs. (8) and (9), we obtain

$$(\bar{H} - E_{CC}) R^k = (E_k - E_{CC}) R^k = \Omega_k R^k, \tag{12}$$

$$L^k (\bar{H} - E_{CC}) = L^k (E_k - E_{CC}) = L^k \Omega_k, \tag{13}$$

$$\Omega_k = E_k - E_{CC}. \tag{14}$$

Therefore, in the matrix form, we have

$$\begin{pmatrix} \bar{H}_{SS} - E_{CC} & \bar{H}_{SD} \\ \bar{H}_{DS} & \bar{H}_{DD} - E_{CC} \end{pmatrix} \begin{pmatrix} R_S^k \\ R_D^k \end{pmatrix} = \Omega_k \begin{pmatrix} R_S^k \\ R_D^k \end{pmatrix}, \tag{15}$$

$$\begin{pmatrix} L_S^k & L_D^k \end{pmatrix} \begin{pmatrix} \bar{H}_{SS} - E_{CC} & \bar{H}_{SD} \\ \bar{H}_{DS} & \bar{H}_{DD} - E_{CC} \end{pmatrix} = \begin{pmatrix} L_S^k & L_D^k \end{pmatrix} \Omega_k. \tag{16}$$

Equations (12) and (13) are solved iteratively by a modified Davidson procedure. This involves calculation of the so-called σ- and $\tilde{\sigma}$-vectors, which are defined as

$$\begin{pmatrix} (\bar{H}_{SS} - E_{CC}) R_S^k + \bar{H}_{SD} R_D^k \\ \bar{H}_{DS} R_S^k + (\bar{H}_{DD} - E_{CC}) R_D^k \end{pmatrix} = \begin{pmatrix} \sigma_S^k \\ \sigma_D^k \end{pmatrix}, \tag{17}$$

$$\begin{pmatrix} L_S^k (\bar{H}_{SS} - E_{CC}) + L_D^k \bar{H}_{DS} & L_S^k \bar{H}_{SD} + L_D^k (\bar{H}_{DD} - E_{CC}) \end{pmatrix} = \begin{pmatrix} \tilde{\sigma}_S & \tilde{\sigma}_D^k \end{pmatrix}. \tag{18}$$

The programmable expressions for the σ- and $\tilde{\sigma}$-vectors are given in Ref. 82.

B. Resolution-of-the-identity and the Cholesky decompositions

In the RI and CD methods, the four-index electron repulsion integrals are replaced by linear combinations of three-index integrals.[54–64,67,83,84] To achieve this, the RI method uses auxiliary bases that are optimized for each primary basis set (and are usually 2-4 times larger than the number of primary basis functions). The CD representation relies on the intrinsic linear dependencies of these four-index electron repulsion integrals. In CD, the three-index integrals are controlled by a single decomposition threshold, δ, which allows one to use any basis set and also to control accuracy. The general implementation of the EOM-CCSD methods using RI and CD representations of the four-index two-electron integrals has been reported earlier.[68] Our programmable expressions for the 2PA cross sections are formulated using the $\tilde{\sigma}$- and σ-vectors (see Appendices A and B); thus, we were able to reuse their RI/CD implementation.[68]

C. Cross sections for two-photon absorption for the exact states

The interaction of molecules with light is described by time-dependent perturbation theory.[85] The unperturbed system is described by the zero-order Hamiltonian, $\hat{H}^{(0)}$, for which the solutions of the Schrödinger equation, the energies E_k and the states $|k\rangle$, are known. The task is then to find the solutions of the perturbed system

$$i \frac{\partial \Psi}{\partial t} = \hat{H} \Psi, \tag{19}$$

$$\hat{H} = \hat{H}^{(0)} + \lambda \hat{V}(t), \tag{20}$$

and to express them in terms of the eigenstates of $H^{(0)}$,

$$\Psi = \sum_n a_n(t) |n\rangle e^{-iE_n t}, \tag{21}$$

$$a_n = a_n^{(0)} + a_n^{(1)} + a_n^{(2)} + \cdots. \tag{22}$$

The Schrödinger equation, Eq. (19), should be satisfied at each order of perturbation. The application of this strategy yields expressions for time-dependent expansion coefficients a_n of Ψ in the basis of zero-order states

$$\frac{\partial a_k^{(0)}}{\partial t} = 0, \tag{23}$$

$$\frac{\partial a_k^{(s+1)}}{\partial t} = \frac{1}{i} \sum_n a_n^{(s)} \langle k | \hat{V}(t) | n \rangle e^{i\Omega_{kn} t}, \tag{24}$$

where $\Omega_{kn} \equiv E_k - E_n$. If initially the system is in state $|0\rangle$, then $a_k^{(0)} = \delta_{k0}$.

In the context of this paper, the perturbation $\hat{V}(t)$ arises from the interaction of the molecular dipole with the external periodic electric fields of the two photons with frequencies ω_b and ω_c,

$$\hat{V}(t) = \vec{\mu} \cdot \vec{E}_0 e^{-i\omega_b t} + \vec{\mu} \cdot \vec{E}_0 e^{-i\omega_c t} = \sum_\alpha \hat{\mu}_\alpha^b E_0^{b\alpha} e^{-i\omega_b t} + \sum_\alpha \hat{\mu}_\alpha^c E_0^{c\alpha} e^{-i\omega_c t}. \tag{25}$$

The $\mu_\alpha^{b,c}$ are the Cartesian components of the electric dipole moment operator. The components of the constant electric field vector, $\vec{E}_0$, are omitted in the subsequent equations. The b-component of the first order coefficient and the bc-component of the second order coefficient are then given by

$$a_{k,b}^{(1)} = -\langle k|\hat{\mu}^b|0\rangle \left(\frac{e^{i(\Omega_{k0}-\omega_b)t}}{\Omega_{k0}-\omega_b}\right), \tag{26}$$

$$a_{k,bc}^{(2)} = -\sum_n \mathcal{P}_{bc}\langle k|\hat{\mu}^c|n\rangle\langle n|\hat{\mu}^b|0\rangle \times \frac{e^{i(\Omega_{k0}-\omega_b-\omega_c)t}}{(\Omega_{n0}-\omega_b)(\omega_b+\omega_c-\Omega_{k0})}, \tag{27}$$

where $\mathcal{P}_{bc}$ symmetrizes indices b and c. As one can see, the coefficients have poles when the perturbing frequency matches the energy spacing ($\Omega_{k0} = \omega_b + \omega_c$) between the zero-order states giving rise to well-known resonance conditions for absorption. From these equations, the cross sections for absorption (that are related to the probability of transitions) can be readily determined giving rise to a familiar sum-over-states expression for the two-photon transition moments

$$M_{bc}^{k\leftarrow 0} = -\sum_n \left(\frac{\langle k|\hat{\mu}^c|n\rangle\langle n|\hat{\mu}^b|0\rangle}{\Omega_{n0}-\omega_b} + \frac{\langle k|\hat{\mu}^b|n\rangle\langle n|\hat{\mu}^c|0\rangle}{\Omega_{n0}-\omega_c}\right), \tag{28}$$

$$M_{bc}^{0\leftarrow k} = -\sum_n \left(\frac{\langle 0|\hat{\mu}^b|n\rangle\langle n|\hat{\mu}^c|k\rangle}{\Omega_{n0}-\omega_b} + \frac{\langle 0|\hat{\mu}^c|n\rangle\langle n|\hat{\mu}^b|k\rangle}{\Omega_{n0}-\omega_c}\right). \tag{29}$$

For the exact states, $M_{bc}^{k\leftarrow 0} = M_{bc}^{0\leftarrow k}$; however for approximate wave functions, the two moments may differ, particularly, for CC methods due to their non-hermitian nature.

Finally, the 2PA cross section, δ^{TPA}, is determined using the components of the transition strength matrix, $S_{ab,cd}$, according to the following equation:[34]

$$\delta^{TPA} = \frac{F}{30}\sum_{a,b} S_{aa,bb} + \frac{G}{30}\sum_{a,b} S_{ab,ab} + \frac{H}{30}\sum_{a,b} S_{ab,ba}, \tag{30}$$

where $S_{ab,cd}$ is given by the product of the left and right 2P transition amplitudes, $M_{ab}^{0\leftarrow f}$ and $M_{cd}^{f\leftarrow 0}$, respectively,

$$S_{ab,cd}^{0f}(\omega) = M_{ab}^{0\leftarrow f}(-\omega)M_{cd}^{f\leftarrow 0}(\omega). \tag{31}$$

The constants F, G, and H depend on the polarization of the incident light. $F = G = H = 2$ for parallel linearly polarized light and $F = -1$, $G = 4$, $H = 1$ for perpendicular linearly polarized light, while $F = -1$, $G = H = 3$ for circularly polarized light. All 2PA cross sections reported in this paper are for parallel linearly polarized light.

The microscopic 2PA cross section, δ^{2PA}, is related to the macroscopic 2PA cross section, σ^{2PA}, according to the equation

$$\sigma^{2PA} = \frac{4\pi^2\alpha a_0^5\omega^2}{c\Gamma}\delta^{2PA}, \tag{32}$$

where α is the fine structure constant, Γ is the lifetime broadening which is set to 0.1 eV in all our calculations (as in the most previous studies), c is the speed of light, a_0 is the Bohr radius, and $\omega^2 = \omega_a \times \omega_b$ is the product of the frequencies of the two photons, i.e., for the resonant degenerate case, Fig. 1(a), $\omega^2 = \frac{E_{ex}^2}{4}$. σ^{2PA} are usually reported in units of GM (Göeppert-Mayer); 1 GM is 10^{-50} cm^4 s/photon.

D. 2PA transition moments for EOM-EE-CCSD states

There are two alternative strategies for formulating calculations of properties and transition probabilities for approximate states.[86] In the so-called response theory formulation, one applies time-dependent perturbation theory to an approximate state (e.g., CCSD wave function); in this approach, the transition moments are defined as residues of the respective response functions. In the expectation-value approach, one begins with the expressions derived for exact states and uses approximate wave functions to evaluate the respective matrix elements. Obviously, the two approaches give the same answer for the exact states (in the full CI case); however, the resulting expressions for approximate states are different.[86] For example, one can compute transition dipole moment for EOM-EE by using expectation value approach; in this case, an unrelaxed one-particle transition density matrix will be used.[52] Alternatively, full response derivation gives rise to the expressions that include amplitude (and, optionally, orbital) relaxation terms (this is how the properties are computed within linear-response formulation of CC theory). Numerically, the two approaches are rather similar, although it should be noted that the expectation-value formulation of properties is not size-intensive[87] (the differences are small in practice[86]).

Here, we employ the expectation-value approach. As the numerical examples below illustrate, the discrepancies between the response theory and the expectation-value formulations are rather small, relative to the errors due to other approximations.

Thus, our starting point is sum-over-state expressions, Eqs. (28) and (29). Of course, sum-over-state expression is impractical for actual calculations, as it entails calculation of all excited states of the system. However, this expression can be easily reformulated using techniques similar to analytic gradient calculations; this will be done in the presentation that follows. A similar strategy was recently used to derive equations for 2PA cross sections within the ADC approach.[43]

Using EOM-CC states, $M_{ab}^{0\leftarrow f}$ assumes the following form:

$$\begin{aligned} M_{ab}^{0\leftarrow f} &= -\sum_n \left(\frac{\langle\Psi_0|\hat{\mu}^a|\Psi_n\rangle\langle\Psi_n|\hat{\mu}^b|\Psi_f\rangle}{\Omega_{n0}-\omega_a} + \frac{\langle\Psi_0|\hat{\mu}^b|\Psi_n\rangle\langle\Psi_n|\hat{\mu}^a|\Psi_f\rangle}{\Omega_{n0}-\omega_b}\right) \\ &= -\sum_n \left(\frac{\langle\Psi_0|\hat{\mu}^a|e^{(\hat{T}_1+\hat{T}_2)}R^n\Phi_0\rangle\langle\Phi_0 L^n e^{-(\hat{T}_1+\hat{T}_2)}|\hat{\mu}^b|\Psi_f\rangle}{\Omega_{n0}-\omega_a} + \frac{\langle\Psi_0|\hat{\mu}^b|e^{(\hat{T}_1+\hat{T}_2)}R^n\Phi_0\rangle\langle\Phi_0 L^n e^{-(\hat{T}_1+\hat{T}_2)}|\hat{\mu}^a|\Psi_f\rangle}{\Omega_{n0}-\omega_b}\right). \end{aligned} \tag{33}$$

Inserting the identity operator ($\hat{1} = \sum_I |\Phi_I\rangle\langle\Phi_I|$) that spans all Slater determinants, we obtain

$$M_{ab}^{0\leftarrow f} = -\sum_n \left(\sum_{IJ} \frac{\langle \Psi_0|\hat{\mu}^a|e^{(\hat{T}_1+\hat{T}_2)}\Phi_I\rangle \langle \Phi_I|R^n\Phi_0\rangle \langle \Phi_0 L^n|\Phi_J\rangle \langle \Phi_J e^{-(\hat{T}_1+\hat{T}_2)}|\hat{\mu}^b|\Psi_f\rangle}{\Omega_{n0}-\omega_a} + \frac{\langle \Psi_0|\hat{\mu}^b|e^{(\hat{T}_1+\hat{T}_2)}\Phi_I\rangle \langle \Phi_I|R^n\Phi_0\rangle \langle \Phi_0 L^n|\Phi_J\rangle \langle \Phi_J e^{-(\hat{T}_1+\hat{T}_2)}|\hat{\mu}^a|\Psi_f\rangle}{\Omega_{n0}-\omega_b} \right), \tag{34}$$

where only the reference (Φ_0), singly (Φ_i^a), and doubly (Φ_{ij}^{ab}) excited determinants survive in EOM-CCSD.

Using the resolvent expression (and exploiting the biorthogonality of left and right EOM states), one can write down

$$\sum_n \frac{\langle \Phi_I|R^n\Phi_0\rangle \langle \Phi_0 L^n|\Phi_J\rangle}{\Omega_{n0}-\omega} = \langle \Phi_I|(\bar{H}-E_{CC}-\omega)^{-1}|\Phi_J\rangle. \tag{35}$$

Consequently, Eq. (34) becomes

$$\begin{aligned} M_{ab}^{0\leftarrow f} &= -\sum_{IJ} (\langle \Psi_0|\hat{\mu}^a|e^{(\hat{T}_1+\hat{T}_2)}\Phi_I\rangle \\ &\quad \times \langle \Phi_I|(\bar{H}-E_{CC}-\omega_a)^{-1}|\Phi_J\rangle \langle \Phi_J e^{-(\hat{T}_1+\hat{T}_2)}|\hat{\mu}^b|\Psi_f\rangle \\ &\quad + \langle \Psi_0|\hat{\mu}^b|e^{(\hat{T}_1+\hat{T}_2)}\Phi_I\rangle \langle \Phi_I|(\bar{H}-E_{CC}-\omega_b)^{-1}|\Phi_J\rangle \\ &\quad \times \langle \Phi_J e^{-(\hat{T}_1+\hat{T}_2)}|\hat{\mu}^a|\Psi_f\rangle) \\ &= -\sum_{IJ} [\tilde{D}^a]_I^0 [(\bar{H}-E_{CC}-\omega_a)^{-1}]_{IJ} [D^b]_J^f \\ &\quad + [\tilde{D}^b]_I^0 [(\bar{H}-E_{CC}-\omega_b)^{-1}]_{IJ} [D^a]_J^f. \end{aligned} \tag{36}$$

Of course, inverting the Hamiltonian is just as impractical as calculating sum-over-states. However, it can be avoided following the strategy similar to gradient calculations,[88] by introducing auxiliary response vectors, $\tilde{X}^a(\omega)$, defined as

$$\tilde{X}^a(\bar{H}-E_{CC}-\omega) = \tilde{D}^a \tag{37}$$

leading to the following expression for transition moments:

$$M_{ab}^{0\leftarrow f} = -\sum_I ([\tilde{X}^a(\omega_a)]_I^0 [D^b]_I^f + [\tilde{X}^b(\omega_b)]_I^0 [D^a]_I^f). \tag{38}$$

We note that the left-hand side of the above equation is almost identical (except for ω) to the equation for the left EOM amplitudes;[68,82] thus, the $\tilde{\sigma}$-vector code for the left EOM eigenvectors can be reused, which greatly simplifies the implementation and validation of both canonical and RI/CD equations. Programmable expressions for the iterative solution of $\tilde{X}^a$ amplitudes are given in the Appendix.

Equivalently, one can solve the response equations using the D^b amplitudes instead of $\tilde{D}^a$ vectors as follows:

$$M_{ab}^{0\leftarrow f} = -\sum_I ([\tilde{D}^a]_I^0 [X^b(\omega_a)]_I^f + [\tilde{D}^b]_I^0 [X^a(\omega_b)]_I^f), \tag{39}$$

where vector $X^a(\omega)$ is defined by the following equation:

$$(\bar{H}-E_{CC}-\omega)X^a = D^a. \tag{40}$$

In this case, the left-hand side of the above equation is similar (except for ω) to the equation for the right EOM amplitudes[68,82] and the σ-vector code for the right EOM eigenvectors can be reused. Programmable expressions for the iterative solution of X^a amplitudes are given in Subsection 2 of the Appendix. The two schemes, one using left response equations ($\tilde{\sigma}$-vectors) and another using right response equations (σ-vectors), are formally and numerically identical.

The $\tilde{D}^\chi$-vector is defined as follows:

$$\begin{aligned} [\tilde{D}^\chi]_I &= \langle \Psi_0|\hat{\mu}^\chi|e^{(\hat{T}_1+\hat{T}_2)}\Phi_I\rangle \\ &= \langle \Phi_0|(\hat{L}_0+\hat{L}_1+\hat{L}_2)e^{-(\hat{T}_1+\hat{T}_2)}\hat{\mu}^\chi e^{(\hat{T}_1+\hat{T}_2)}|\Phi_I\rangle, \end{aligned} \tag{41}$$

where $\chi = x$, y, or z and I denotes the excitation level (O, S, or D).

Note that $L_0 = 1$ for the CCSD ground state (and L_1 and L_2 are commonly denoted as Λ_1 and Λ_2; they are found by solving CCSD response equations) and $L_0 = 0$ for the EOM-CCSD states. Similarly, the D^χ-vector is

$$\begin{aligned} [D^\chi]_I &= \langle \Phi_I e^{-(\hat{T}_1+\hat{T}_2)}|\hat{\mu}^\chi|\Psi_f\rangle \\ &= \langle \Phi_I e^{-(\hat{T}_1+\hat{T}_2)}|\hat{\mu}^\chi|(\hat{R}_0+\hat{R}_1+\hat{R}_2)e^{\hat{T}_1+\hat{T}_2}\Phi_0\rangle. \end{aligned} \tag{42}$$

Appendices A 3 and A 4 provide the programmable expressions for these $\tilde{D}^\chi$ and D^χ intermediates, respectively.

Following the same strategy, we eliminate the sum-over-states in the right transition amplitudes, Eq. (28), arriving at

$$\begin{aligned} M_{ab}^{f\leftarrow 0} &= -\sum_{IJ} [\tilde{D}^b]_I^f [(\bar{H}-E_{CC}-\omega_a)]_{IJ} [D^a]_J^0 \\ &\quad + [\tilde{D}^a]_I^f [(\bar{H}-E_{CC}-\omega_b)]_{IJ} [D^b]_J^0 \\ &= -\sum_I ([\tilde{X}^b(\omega_a)]_I^f [D^a]_I^0 + [\tilde{X}^a(\omega_b)]_I^f [D^b]_I^0) \end{aligned} \tag{43}$$

by solving the left response equations or at

$$M_{ab}^{f\leftarrow 0} = -\sum_I ([\tilde{D}^b]_I^f [X^a(\omega_a)]_I^0 + [\tilde{D}^a]_I^f [X^b(\omega_b)]_J^0) \tag{44}$$

by solving the right response equations. The right and the left transition amplitudes can then be combined together to obtain the transition strengths and the 2PA cross sections using Eqs. (31) and (30).

E. Implementation

The programmable expressions for 2PA cross sections using EOM-EE-CCSD states were implemented in a development version of Q-Chem,[44,45] using our recently developed libtensor library.[89] The code for EOM σ-vectors was reused in the response equations; this greatly simplified the implementation and validation of the canonical and the RI/CD versions.[68,82] Similarly to EOM-CCSD energy calculations, the RI/CD implementation of 2PA cross sections avoids the creation and storage of bulky two-electron integrals and intermediates that significantly reduces storage requirements and IO penalties leading to better parallel performance. The specific gains depend, of course, on the architecture, e.g., the gains will

be smaller for fast solid state drives than for raided SAS or SATA HDDs.

The canonical implementation was validated against calculations of 2PA transition moments using the sum-over-states expressions, Eqs. (29) and (28), for $1A_1$ and $2A_1$ states of HeH^+ and $1A_1$ excited state of H_2O with the STO-3G basis set. The details of these calculations as well as raw data are given in the supplementary material.[90] The differences between analytical transition moments and the sum-over-states values did not exceed 0.3%. For a two-electron system, the expectation-value and linear response calculations should yield the identical results. Indeed, for HeH^+, the EOM-EE transition strength computed by Q-Chem and linear response value computed by Dalton agree up to 4 decimal points (the difference is 7.6×10^{-5}%). The numeric agreement (up to sixth decimal point) between the cross sections computed with two different schemes, either using left or right response equations (with $\tilde{\sigma}$- or σ-vectors, respectively), provides additional validation of our implementation (see Table S11 of the supplementary material[90]).

The validation of RI/CD implementation is straightforward—identical results should be obtained from the full RI/CD implementation and a canonical implementation that uses the two-electron integrals reconstructed from the respective decomposed forms.

Our implementation allows for two different types of calculations. The default case is the absorption of two degenerate photons each with an energy equal to half the energy difference between the initial and final states, see Fig. 1(a). The second case is the absorption of two non-degenerate photons that satisfy the resonance condition for the excited state. The user can also provide a range of frequencies for the first photon (the frequency of the second is then computed based on the energy gap between the initial and final states) and scan the 2PA cross sections across this spectrum. Our implementation also allows one to compute cross sections for transitions between excited states (EOM-EOM 2PA); see supplementary material for further details.[90]

The present implementation cannot reliably handle resonance-enhanced 2PA calculations due to singularities in the response equations, Eqs. (37) and (40), that cause convergence problems. Damped response theory has been previously used to address this issue by inclusion of an empirical damping term, which brings the singularity into the complex plane and results in a well-behaved convergence of the iterative solution of the response equations.[91,92] We will pursue a similar approach in future work.

III. COMPUTATIONAL DETAILS

We begin by considering several small molecules (water, formaldehyde, and diacetylene) for which extensive benchmark data are available.[34] The goal of our benchmark calculations was three-fold. First, using benchmark data from Ref. 34, we compared our expectation-value formulation of 2PA against full quadratic response CCSD calculations. In order to assess accuracy, both theories were compared against a higher level coupled-cluster method, CC3. Second, we quantified the errors due to RI/CD representations by comparing against the canonical implementation. Third, we investigated whether the requirements to basis sets can be relaxed by removing higher angular momentum functions from the augmenting sets. For selected examples, we also investigated computational costs of 2PA calculations as well as computational savings due to using RI/CD.

The geometries and basis sets[93–95] were the same as in Ref. 34 (also provided in the supplementary material[90]). Pure angular momentum was used in Dunning's basis sets. All electrons were active in these calculations, to enable direct comparison with Ref. 34.

In the RI calculations with cc-pVXZ, aug-cc-pVXZ, and d-aug-cc-pVXZ (X = D,T,Q), the standard MP2-optimized auxiliary basis sets were employed.[67,96] The CD calculations employed two thresholds: 10^{-4} (which was shown to yield negligible errors in excitation energies[68]) as well as more aggressive 10^{-2}. Note that in our implementation, the CD is invoked only in post-Hartree-Fock calculations; the SCF equations are solved using full two-electron integrals.

In the calculations investigating basis set effects, we performed EOM-EE-CCSD calculations for these three molecules with singly and doubly augmented Dunning bases modified by sequential removal of the g, f, d, and p functions from the augmenting sets.

Finally, to illustrate the capabilities of the new method, we performed calculations for several larger systems, such as model chromophores of GFP and PYP. In these calculations, we employed CD-EOM-EE-CCSD with a threshold of 10^{-2} that affords significant computational savings; core electrons were frozen. Dunning's d-aug-cc-pVDZ basis set with the d-functions removed from the second augmenting set was used in these calculations. The geometries for model PYP and GFP chromophores were optimized by RI-MP2 with the aug-cc-pVDZ and aug-cc-pVTZ bases, respectively. We considered only the neutral forms of these chromophores. The chromophores have C_s symmetry. We computed 2PA cross sections for the lowest two A′ and A″ excited states for each chromophore.

IV. RESULTS AND DISCUSSION

A. 2PA cross sections for EOM-EE-CCSD

The results of benchmark calculations for water, formaldehyde, and diacetylene are presented in Figs. 2 and 3; the respective raw data are given in the supplementary material (Tables S3-S5).[90]

For water (5 excited states), the mean average deviation (MAD, in %) of EOM-EE-CCSD versus quadratic response CCSD computed in all bases is about 2%; and the standard deviation is ~1.2% (Fig. 2). Thus, expectation-value formulation of 2PA cross sections for CCSD yields the results that are very close to those obtained within response theory.

MAD against CC3 response is about 2%-3% with large standard deviations of about 7%-8%. The analysis of the raw data (see Table S3[90]) reveals that the primary contribution to this discrepancy comes from the $1A_1$ state (and only in doubly augmented basis sets). It is not clear why triple excitations appear to be important for this particular state (which has a clear singly excited character). It would be interesting to

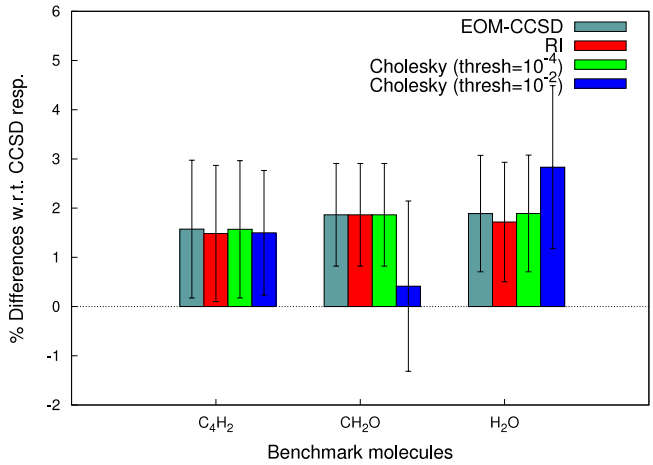

FIG. 2. Comparison of 2PA cross sections computed with (RI/CD)-EOM-EE-CCSD against CCSD response theory. Bars and lines denote mean average deviation and standard deviation, respectively.

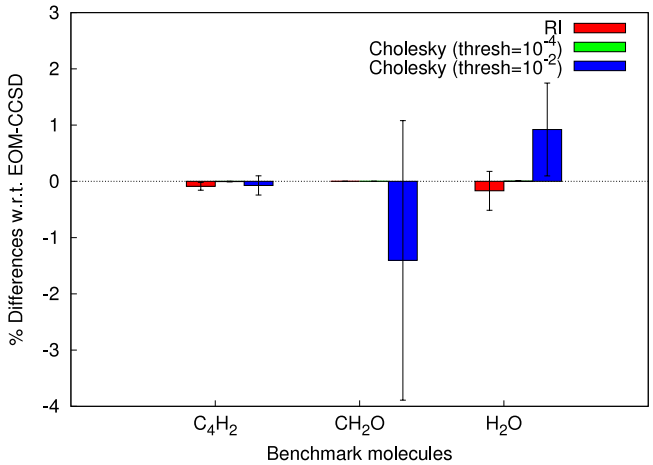

FIG. 4. Comparison of 2PA cross sections computed with RI/CD implementation of EOM-EE-CCSD against the canonical version. Bars and lines denote mean average deviation and standard deviation, respectively.

compare CC3 with explicit triples (CCSDT) calculations. If we exclude the results for this outlier state (in doubly augmented bases), the MAD is reduced to about 0.3% with standard deviation of less than 3% (Fig. 3).

Similarly, for the $1A_2$ state of formaldehyde, the MAD of EOM-EE-CCSD versus quadratic response CCSD is about 2% across all bases. However, MAD against CC3 response is much larger (with standard deviations more than 50%). The analysis of the data reveals that the unaugmented bases, cc-pVXZ, predict relatively small cross sections and small deviation in the absolute cross sections relative to the CC3 response theory contributes a large percent deviation to the MAD and the standard deviation. If the results of these small bases (that were shown[34] to lead to large errors in 2PA cross sections) are excluded from the analysis, the MAD and standard deviations of EOM-EE-CCSD versus CC3 are reduced to 5%-9%.

The results for the $1\Pi_g$ of diacetylene follow similar trends. MADs of EOM-EE-CCSD versus quadratic response CCSD and CC3 are about 3% and −5%, respectively, with standard deviations of about 3% and 7%, respectively. Excluding the artifacts due to use of unaugmented basis, cc-pVXZ, the MADs of EOM-EE-CCSD versus quadratic response CCSD and CC3 are about 2% and −9%, respectively, with standard deviations of about 1% and 2%, respectively (Figs. 2 and 3).

Fig. 4 shows how 2PA cross sections with RI-EOM-EE-CCSD and CD-EOM-EE-CCSD compare against the canonical EOM-EE-CCSD results across all the excited states of the three molecules studied here (the raw data are given in the supplementary material, Tables S3-S5[90]). The RI and CD approximations (with threshold of 10^{-4}) introduce negligible errors. This is very encouraging, in view of the need for large heavily augmented basis set for obtaining converged results. Thus, RI/CD efficiently removes linear dependencies while preserving important features of the extended bases. This allows one to obtain reliable 2PA cross sections for a reduced cost. We note that even when using a very aggressive threshold of 10^{-2}, the maximum MAD is less than 1.5% with a standard deviation of less than 2.5%.

The results for water, formaldehyde, and diacetylene with the modified bases are shown in Figs. 5–7 (the raw data are given in the supplementary material, Tables S6-S8[90]). As one

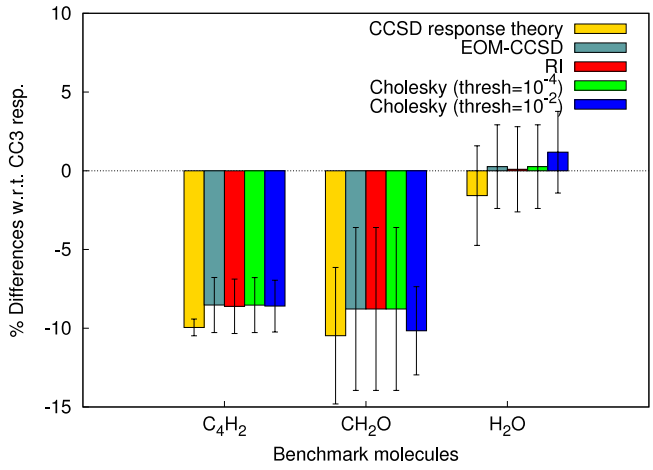

FIG. 3. Comparison of 2PA cross sections computed with (RI/CD)-EOM-EE-CCSD against CC3 response theory. Bars and lines denote mean average deviation and standard deviation, respectively.

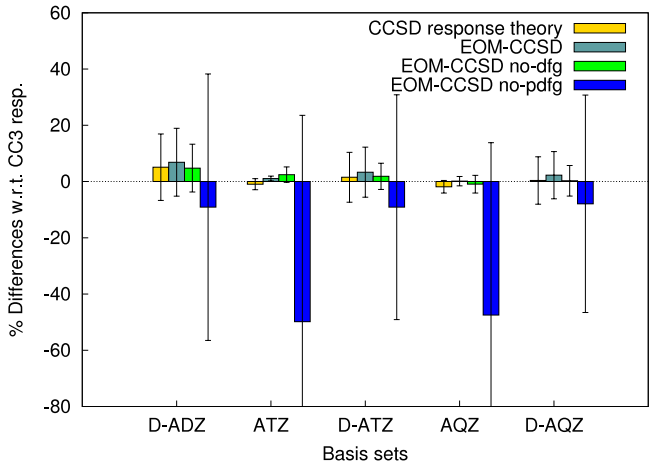

FIG. 5. Performance of Dunning bases (aug-cc-pVXZ and d-aug-cc-pVXZ (X = D, T, Q)) modified by removing the g, f, d, and p functions from the last augmenting set in calculations of the 2PA cross sections of the $1A_1$, $2A_1$, $1B_2$, $2B_2$, and $1A_2$ excited states of H_2O. Bars and lines denote mean average deviation and standard deviation, respectively.

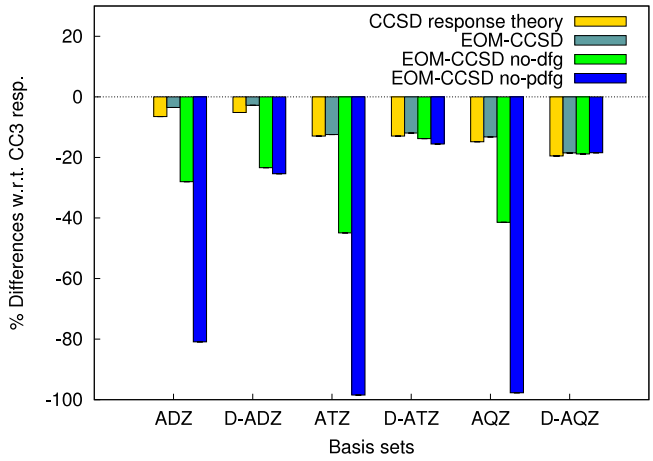

FIG. 6. Performance of Dunning bases (aug-cc-pVXZ and d-aug-cc-pVXZ (X = D, T, Q)) modified by removing the g, f, d, and p functions from the last augmenting set in calculations of the 2PA cross section of the $1A_2$ excited state of CH_2O.

can see for water example, the removal of the d, f, and g functions from the last augmenting set for the singly and doubly augmented Dunning bases does not introduce significant errors, but the subsequent removal of the p functions introduces large errors.

The results for formaldehyde are similar—the removal of d, f, and g functions from the second augmenting set in d-aug-cc-pVXZ introduces negligible errors, with an exception of the d-aug-cc-pVDZ basis where the d-functions are important. This is primarily due to the fact that the 2PA cross sections are not converged with the d-aug-cc-pVDZ basis, which has been emphasized in Ref. 34. We note that the removal of d, f, and g functions from the augmenting set in the singly augmented Dunning basis sets in formaldehyde introduces non-negligible errors which again emphasizes the importance of at least one full augmenting set. The subsequent removal of the p-functions from the doubly augmented basis sets, however, introduces negligible errors, which again supports the fact that in this case the 2PA cross sections are sufficiently converged with the singly augmented basis sets (except the d-aug-cc-pVDZ basis set).

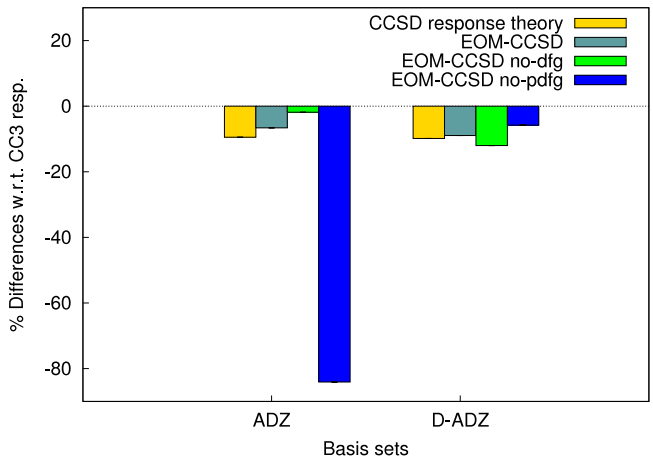

FIG. 7. Performance of Dunning bases (aug-cc-pVXZ and d-aug-cc-pVXZ (X = D, T, Q)) modified by removing the g, f, d, and p functions from the last augmenting set in calculations of the 2PA cross section of the $1\Pi_g$ excited state of C_4H_2.

Similarly, for the $1\Pi_g$ state of diacetylene, the removal of p, d, f, and g functions from the second augmenting set for the doubly augmented Dunning basis sets introduces negligible errors; but the p functions are important in singly augmented Dunning bases.

In sum, one can safely use these modified bases (d-aug-cc-pVXZ-dfg) for 2PA calculations. Removing p-functions is not recommended. Moreover, CD-EOM-EE-CCSD calculation with a loose Cholesky threshold of 10^{-2} can be employed leading to significant computational savings while introducing relatively small errors (<4% relative to canonical EOM-EE-CCSD). Thus, in calculations of 2PA cross sections in large chromophores, we employ CD-EOM-EE-CCSD (threshold of 10^{-2}) with the modified d-aug-cc-pVDZ basis set from which the d-functions were removed from the second augmenting set.

Finally, to assess numerical consequences of the lack of size-extensivity in EOM properties formulated using expectation-value approach, we performed the following calculations using two model systems. Our first system was diacetylene to which 1, 2, and 3 He atoms were added at large distances. In this system, the lowest excited states are localized on diacetylene. We considered 10 lowest excited states (4 pairs of Π states and 2 Σ state). The computed excitation energies, transition dipole, and 2PA moments were unaffected by helium atoms (the differences were within numeric noise, 0.001%-0.002%). We then considered a more interesting example,[87] two non-interacting chromophores, $(LiH)_2$. In this case, the excited states of the dimer are linear combinations of the monomers' states. The energies of these states are exactly the same as in the monomer (within 0.002%). We observe that the corresponding one and two-photon cross sections of the dimer differ by 0.4% and 5%, respectively. Thus, the lack of size extensivity in the expectation-value formulation of properties only manifests itself in a system of multiple chromophores with delocalized excited states (and not in a localized chromophore embedded in a system of an increasing size).

B. 2PA cross sections of PYP and GFP chromophores

In this section, we illustrate the capabilities of the new code by computing 2PA cross sections for model chromophores of PYP and GFP. Our results represent the highest-level of theory 2PA calculations for these systems reported so far. Structures of the neutral chromophores of PYP and GFP are shown in Fig. 8; the respective Cartesian coordinates are given in the supplementary material.[90] 2PA cross sections for the two lowest A′ and A″ excited states of the neutral PYP chromophore and the lowest A′ and A″ excited states of the neutral GFP chromophore are given in Tables I and II, respectively. As expected from the selection rules for the C_s point group, bright A′ states in one-photon spectroscopy have large 2PA cross sections, while the A″ states have small 2PA cross sections for both chromophores.

The comparison of the computed cross sections with experimental values is not straightforward. For PYP, absolute 2PA cross sections have not yet been reported. For GFP, the reported values range from a few GM to almost 200

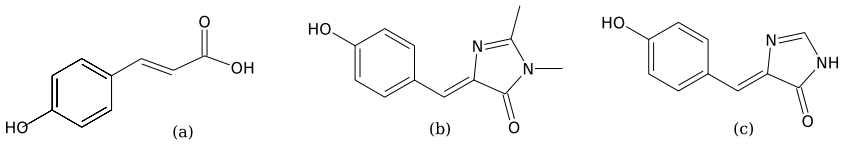

FIG. 8. Model chromophores of (a) PYP, (b) GFP (HBDI), and (c) GFP (HBI).

GM.[27,97–99] It should be noted, that unlike excitation energies and one-photon oscillator strengths, 2PA cross sections seem to depend strongly on the environment. For example, the experimental 2PA cross sections of red fluorescent proteins with identical DsRed-like chromophores (DsRed, mCherry, and mStrawberry) differ by a factor of 5.[100] Calculations of 2PA cross sections of GFP using TDDFT within quantum mechanics/molecular mechanics and polarizable embedding schemes have illustrated that the cross section changes by a factor of 2 (or even more, depending on the level of theory) when nearby water molecules and the protein environment is included in the calculation.[32]

For the first bright 2PA transition of the model neutral GFP chromophore (4′-hydroxybenzylidene-2,3-dimethylimidazoline or HBDI), we report a 2PA cross section of 5.64 GM with an excitation energy of 3.97 eV and oscillator strength of 0.77. A TDDFT response calculations[101] of this model chromophore using the B3LYP functional and 6-31+G*(6-31G*) bases yielded a gas-phase 2PA cross section of 5.58 GM (6.14 GM) with an excitation energy of 3.46 eV (3.54 eV) and oscillator strength of 0.69 (0.70). Similar-magnitude cross section (7.76 GM) has been obtained with CAM-B3LYP/6-31+G* by Kongsted and coworkers.[32] No CC values for this model chromophore have been reported. However, for a similar model chromophore (4′-hydroxybenzylidene-imidazoline or HBI), CC2/6-31+G* calculations were performed; the reported cross section was around 80 GM.[38] To clarify such large discrepancy, we performed calculations for HBI using the same basis set. The CD-EOM-CCSD/6-31+G* (thresh = 10^{-2}) cross section is 18.3 GM. Using a better basis set, the modified d-aug-cc-pVDZ basis set (with core electrons frozen), 2PA cross section of 14.68 GM was obtained. Thus, for the same model chromophore and basis set, the reported[38] CC2 cross section is 4.4 times larger that the EOM-CCSD one (and TDDFT). Thus, it appears that CC2 strongly overestimates 2PA cross sections, compared to a higher-level EOM-CCSD.[102] We note that large differences (about a factor of 9) between TDDFT/CAM-B3LYP and CC2 2PA cross sections were observed in the calculations of yellow fluorescent protein.[21]

TABLE I. 2PA cross sections at $\omega_1 = \omega_2 = \frac{E_{ex}}{2}$ for the neutral chromophore of PYP calculated with CD-EOM-EE-CCSD (thresh = 10^{-2}) and a modified d-aug-cc-pVDZ basis from which the second-set augmenting d-functions were removed.

	Calc.		
Excited state	E_{ex}, eV	Oscil. str., a.u.	δ^{2PA}, a.u.
1A′	4.4842	0.218	1224.224
2A′	4.7491	0.525	2631.175
1A″	5.0711	0.000	0.057
2A″	5.4509	0.000	3.365

C. Computational performance

Here, we analyze computational costs of 2PA cross section calculations. In order to compute transition properties, one needs to compute both left and right EOM amplitudes; this roughly doubles the cost (relative to energy calculation that only requires right EOM amplitudes). 2PA cross sections also require solving auxiliary response equations, Eqs. (37) and (40), which are similar in complexity to σ-vector evaluations (6 for each target state).

Detailed timings for various steps in 2PA cross sections' calculations are collected in the supplementary material[90] (Tables S9 and S10) for the lowest A″ state of the PYP chromophore in the aug-cc-pVDZ basis. As expected, the two schemes, i.e., using left or right response equations, yield numerically identical (up to fifth decimal point) 2PA cross sections. Thus, the choice of using $\tilde{\sigma}$- or σ-vectors in response calculations depends on the computational cost of these calculations. Both schemes scale as N^6; however, the number of rate-determining contractions is slightly different; also, $\tilde{\sigma}$ and σ equations use slightly different sets of intermediates (transformed integrals).

As one can see from the timings for right and left EOM vectors, in the canonical implementation the timings for left vectors are slightly faster. Consequently, the scheme using left response equations ($\tilde{\sigma}$-intermediates) is faster (about 10%); thus, this scheme is recommended for canonical calculations of 2PA cross sections. Overall, the additional cost of 2PA cross sections is about 10 times of that of calculating EOM states and one-photon transition moments.

The picture, however, is different for the RI/CD implementation in which the most expensive 4-index intermediates are re-assembled at each iteration.[68] Even though the canonical and RI/CD implementations have the same scaling, the number of N^6 contractions differs. For example, the canonical σ-vector calculation only involves three N^6 contractions, against seven N^6 contractions in RI/CD σ-vector calculation.[68] The increased number of floating point operations offsets the gains due to reduced I/O. While for the right EOM amplitude calculations (dominated by σ-vector updates), there is an overall gain (1.6-1.8 speedup),

TABLE II. 2PA cross sections at $\omega_1 = \omega_2 = \frac{E_{ex}}{2}$ for the neutral chromophore (HBDI) of GFP calculated with CD-EOM-EE-CCSD (thresh = 10^{-2}) and a modified d-aug-cc-pVDZ basis from which the second-set augmenting d-functions were removed.

	Calc.		
Excited state	E_{ex}, eV	Oscil. str., a.u.	δ^{2PA}, a.u.
1A′	3.9667	0.772	977.762
1A″	4.2913	0.001	0.013

the calculations of the left EOM amplitudes (dominated by $\tilde{\sigma}$-vector updates) are about a factor of 2 slower in the RI/CD implementation.

Consequently, the RI/CD 2PA calculations are slower than the canonical implementation when left response equations ($\tilde{\sigma}$-vectors) are used. However, using right response equations leads to a moderate gain (1.2-1.4 speedup) relative to the respective canonical calculation. Thus, this scheme is recommended for 2PA calculations using RI/CD. It should be pointed out that the main advantage of the RI/CD implementation is in reducing disk storage requirements. Also, due to increased parallel scaling, larger gains are expected for larger systems and with more processors. Of course, the I/O penalties can be reduced by using faster storage, such as, for example, solid state drives. Thus, the choice of optimal algorithm depends on the hardware configuration. In order to achieve further gains, additional steps should be taken. Among promising strategies[59] is a tensor hyper-contraction approach.[83,84]

V. CONCLUSIONS

We presented a formalism and a new computer implementation for calculating 2PA cross sections using EOM-CCSD wave functions. We exploit expectation-value approach in which properties are computed using the expressions derived for exact states and approximate wave functions. The comparison of canonical EOM-CCSD against an alternative formulation via response theory shows that the numeric differences between two approaches are about 0%−<3%.

As far as the comparison against higher-level CC methods is concerned, the differences between EOM-CCSD and CC3 are within 10% for most cases.

The cross sections require calculations of left EOM eigenstates (as in calculations of a gradient or one-photon transition moments) as well as solving auxiliary response equations that are similar to σ-vector evaluations (6 additional equations for each target state and each frequency need to be solved). Thus, the additional computational costs of 2PA cross sections' calculation relative to regular transition dipole moments roughly equal 6-10 times that of calculating EOM states and one-photon transition moments.

In addition to the canonical implementation, we report an implementation using RI/CD representations of electron repulsion integrals. This allows for significant reductions of the disk storage requirements and I/O overheads which improves parallel performance. Importantly, the numerical errors due to RI/CD approximations are less than 4%, which is very encouraging in view of large basis set requirements for calculating 2PA cross sections. We illustrate the capabilities of the new code by calculations of 2PA cross sections for model chromophores of PYP and GFP.

ACKNOWLEDGMENTS

A.I.K. acknowledges support by the U.S. National Science Foundation (No. CHE-1264018).

APPENDIX: PROGRAMMABLE EXPRESSIONS

1. Iterative scheme for the $\tilde{X}^{\chi}$ amplitudes

$$[\tilde{X}^{\chi}]_0 = -\frac{[\tilde{D}^{\chi}]_0}{\omega}, \tag{A1}$$

$$[\tilde{X}^{\chi}]_S^{(n+1)} = \frac{[\tilde{D}^{\chi}]_S - [\tilde{X}^{\chi}]_0 \bar{H}_{OS} - \tilde{\sigma}_1 + [\tilde{X}^{\chi}]_S^{(n)}\omega}{\bar{H}^d_{SS} - E_{CC} - \omega} + [\tilde{X}^{\chi}]_S^{(n)}, \tag{A2}$$

$$[\tilde{X}^{\chi}]_D^{(n+1)} = \frac{[\tilde{D}^{\chi}]_D - [\tilde{X}^{\chi}]_0 \bar{H}_{OD} - \tilde{\sigma}_2 + [\tilde{X}^{\chi}]_D^{(n)}\omega}{\bar{H}^d_{DD} - E_{CC} - \omega} + [\tilde{X}^{\chi}]_D^{(n)}, \tag{A3}$$

$$[H_{OS}]_i^a = \langle \Phi_0 | \bar{H} | \Phi_i^a \rangle = f_{ia} + \sum_{jb} t_j^b \langle ij||ab\rangle, \tag{A4}$$

$$[H_{OD}]_{ij}^{ab} = \langle \Phi_0 | \bar{H} | \Phi_{ij}^{ab} \rangle = \langle ij||ab\rangle. \tag{A5}$$

Expressions for $\bar{H}^d_{SS}$ and $\bar{H}^d_{DD}$ (diagonals of SS and DD blocks of $\bar{H}$) are given in Ref. 82.

2. Iterative scheme for the X^{χ} amplitudes

$$[X^{\chi}]_0 = \frac{[D^{\chi}]_0 - \bar{H}_{0S}[X^{\chi}]_s - \bar{H}_{0D}[X^{\chi}]_D}{-\omega}, \tag{A6}$$

$$[X^{\chi}]_S^{(n+1)} = \frac{[D^{\chi}]_S - \sigma_S + \omega[X^{\chi}]_S^{(n)}}{\bar{H}^d_{SS} - E_{CC} - \omega} + [X^{\chi}]_S^{(n)}, \tag{A7}$$

$$[X^{\chi}]_D^{(n+1)} = \frac{[D^{\chi}]_D - \sigma_D + \omega[X^{\chi}]_D^{(n)}}{\bar{H}^d_{DD} - E_{CC} - \omega} + [X^{\chi}]_D^{(n)}. \tag{A8}$$

3. Expressions for $\tilde{D}^{\chi}$ intermediates

$l_0 = 1$ for the reference CCSD wave function
$l_0 = 0$ for all EOM excited states
$r_0 = 1$ for the reference CCSD wave function
$r_0 = \frac{1}{\Omega}\left(\sum_{ia} r_i^a f_i^a + \sum_{ijab} r_i^a t_j^b \langle ij||ab\rangle + \frac{1}{4} r_{ij}^{ab} \langle ij||ab\rangle\right)$
for an EOM excited state with excitation energy Ω,

$$\begin{aligned}
[\tilde{D}^{\chi}]_0 &= \langle \Phi_0 (\hat{L}_0 + \hat{L}_1 + \hat{L}_2) e^{-(\hat{T}_1+\hat{T}_2)} | \hat{\mu}^{\chi} | e^{(\hat{T}_1+\hat{T}_2)} \Phi_0 \rangle \\
&= Tr[\mu^{\chi}_{oo}] l_0 - \sum_{ij} \mu^{\chi}_{ij} \left[\sum_a l_j^a t_i^a + \frac{1}{2} \sum_{kab} l_{jk}^{ab} t_{ik}^{ab} \right] \\
&\quad + \sum_{ia} \mu^{\chi}_{ia} \left[l_i^a + l_0 t_i^a + \sum_{jb} l_j^b (t_{ij}^{ab} - t_i^b t_j^a) \right. \\
&\quad \left. + \frac{1}{2} \sum_{jkbc} L_{jk}^{bc} t_i^c t_{jk}^{ab} + \frac{1}{2} \sum_{jkbc} L_{jk}^{bc} t_k^a t_{ij}^{bc} \right] \\
&\quad + \sum_{ab} \mu^{\chi}_{ab} \left[\sum_i l_i^a t_i^b + \frac{1}{2} \sum_{ijc} l_{ij}^{ac} t_{ij}^{bc} \right],
\end{aligned} \tag{A9}$$

$$\begin{aligned}
[\tilde{D}^{\chi}]_S &= [\tilde{D}^{\chi}]_k^c \\
&= \langle \Phi_0 (\hat{L}_0 + \hat{L}_1 + \hat{L}_2) e^{-(\hat{T}_1+\hat{T}_2)} | \hat{\mu}^{\chi} | e^{(\hat{T}_1+\hat{T}_2)} \Phi_c^k \rangle \\
&= -\sum_j \mu^{\chi}_{kj} l_j^c + Tr[\mu^{\chi}_{oo}] l_k^c + \mu^{\chi}_{kc} l_0
\end{aligned}$$

$$
\begin{aligned}
&- \sum_{ij} \mu^{\chi}_{ij} \sum_{a} l^{ac}_{jk} t^{a}_{i} + \sum_{ai} \mu^{\chi}_{ai} \\
&\times \left[l^{ac}_{ik} + l^{c}_{k} t^{a}_{i} + \sum_{jb} l^{bc}_{jk} (t^{ab}_{ij} - t^{b}_{i} t^{a}_{j}) \right] \\
&+ \sum_{a} \mu^{\chi}_{ac} l^{a}_{k} + \sum_{a} \mu^{\chi}_{ka} \left[\frac{1}{2} \sum_{jlb} l^{bc}_{jl} t^{ab}_{jl} - \sum_{j} l^{c}_{j} t^{a}_{j} \right] \\
&+ \sum_{ab} \mu^{\chi}_{ab} \sum_{i} l^{ac}_{ik} t^{b}_{i} \\
&+ \sum_{i} \mu^{\chi}_{ic} \left[\frac{1}{2} \sum_{jbd} l^{bd}_{jk} t^{bd}_{ij} - \sum_{b} l^{b}_{k} t^{b}_{i} \right], \qquad \text{(A10)}
\end{aligned}
$$

$$
\begin{aligned}
[\tilde{D}^{\chi}]_D &= [\tilde{D}^{\chi}]^{cd}_{kl} \\
&= \langle \Phi_0 (\hat{L}_0 + \hat{L}_1 + \hat{L}_2) e^{-(\hat{T}_1 + \hat{T}_2)} | \hat{\mu}^{\chi} | e^{(\hat{T}_1 + \hat{T}_2)} \Phi^{kl}_{cd} \rangle \\
&= \mathcal{P}^{-}_{cd} \mathcal{P}_{kl} \mu^{\chi}_{ld} l^{c}_{k} + \mathcal{P}^{-}_{kl} \sum_{j} \mu^{\chi}_{lj} l^{cd}_{jk} \\
&\quad + \mathcal{P}^{-}_{cd} \sum_{a} \mu^{\chi}_{ac} l^{ad}_{kl} + \mathcal{P}^{-}_{cd} \sum_{i} \mu^{\chi}_{id} \sum_{b} l^{bc}_{kl} t^{b}_{i} \\
&\quad + \mathcal{P}^{-}_{kl} \sum_{a} \mu^{\chi}_{la} \sum_{j} l^{cd}_{jk} t^{a}_{j} \\
&\quad + \sum_{ia} \mu^{\chi}_{ia} l^{cd}_{kl} t^{a}_{i} + Tr[\mu^{\chi}_{oo}] l^{cd}_{kl}. \qquad \text{(A11)}
\end{aligned}
$$

4. Expressions for D^{χ} intermediates

$$
\begin{aligned}
[D^{\chi}]_0 &= \langle \Phi_0 e^{-(\hat{T}_1 + \hat{T}_2)} | \hat{\mu}^{\chi} | (\hat{R}_0 + \hat{R}_1 + \hat{R}_2) e^{(\hat{T}_1 + \hat{T}_2)} \Phi_0 \rangle \\
&= Tr[\mu^{\chi}_{oo}] r_0 + \sum_{ia} \mu^{\chi}_{ia} \left[r^{a}_{i} + r_0 t^{a}_{i} \right], \qquad \text{(A12)}
\end{aligned}
$$

$$
\begin{aligned}
[D^{\chi}]_S &= [D^{\chi}]^{c}_{k} \\
&= \langle \Phi^{c}_{k} e^{-(\hat{T}_1 + \hat{T}_2)} | \hat{\mu}^{\chi} | (\hat{R}_0 + \hat{R}_1 + \hat{R}_2) e^{(\hat{T}_1 + \hat{T}_2)} \Phi_0 \rangle \\
&= \mu^{\chi}_{ck} r_0 - \sum_{i} \mu^{\chi}_{ik} \left[r^{c}_{i} + t^{c}_{i} r_0 \right] \\
&\quad + Tr[\mu^{\chi}_{oo}] r^{c}_{k} + \sum_{b} \mu^{\chi}_{cb} \left[r^{b}_{k} + t^{b}_{k} r_0 \right] \\
&\quad + \sum_{ia} \mu^{\chi}_{ia} \left[r^{ac}_{ik} + t^{ac}_{ik} r_0 + \mathcal{P}^{-}_{ki} r^{c}_{k} t^{a}_{i} - r^{a}_{k} t^{c}_{i} - t^{a}_{k} t^{c}_{i} r_0 \right], \qquad \text{(A13)}
\end{aligned}
$$

$$
\begin{aligned}
[D^{\chi}]_D &= [D^{\chi}]^{cd}_{kl} \\
&= \langle \Phi^{cd}_{kl} e^{-(\hat{T}_1 + \hat{T}_2)} | \hat{\mu}^{\chi} | (\hat{R}_0 + \hat{R}_1 + \hat{R}_2) e^{(\hat{T}_1 + \hat{T}_2)} \Phi_0 \rangle \\
&= \mathcal{P}^{-}_{cd} \mathcal{P}^{-}_{kl} \mu^{\chi}_{dl} r^{c}_{k} + \mathcal{P}^{-}_{kl} \sum_{i} \mu^{\chi}_{ik} \\
&\quad \times \left[-r^{cd}_{il} - t^{cd}_{il} r_0 + \mathcal{P}^{-}_{cd} r^{c}_{l} t^{d}_{i} \right] \\
&\quad + Tr[\mu^{\chi}_{oo}] r^{cd}_{kl} + \mathcal{P}^{-}_{cd} \sum_{b} \mu^{\chi}_{db} \\
&\quad \times \left[-r^{bc}_{kl} - t^{bc}_{kl} r_0 + \mathcal{P}^{-}_{kl} r^{c}_{k} t^{b}_{l} \right] \\
&\quad + \sum_{ia} \mu^{\chi}_{ia} [r^{cd}_{kl} t^{a}_{i} + \mathcal{P}^{-}_{kl} (r^{cd}_{ik} t^{a}_{l} + t^{cd}_{ik} r^{a}_{l}) \\
&\quad + \mathcal{P}^{-}_{cd} (r^{ac}_{kl} t^{d}_{i} + t^{ac}_{kl} r^{d}_{i}) + \mathcal{P}^{-}_{kl} \mathcal{P}^{-}_{kl} t^{ad}_{il} r^{c}_{k} + \mathcal{P}^{-}_{kl} t^{cd}_{ik} t^{a}_{l} r_0 \\
&\quad + \mathcal{P}^{-}_{cd} t^{ac}_{kl} t^{d}_{i} r_0 + \mathcal{P}^{-}_{cd} t^{c}_{i} (\mathcal{P}^{-}_{kl} r^{d}_{k} t^{a}_{l})]. \qquad \text{(A14)}
\end{aligned}
$$

The terms involving the trace of μ_{oo} contribute only when the dipole operator has totally symmetric irreducible representation, otherwise the trace is zero. The terms involving l_0 are only computed when l_0 is non-zero (e.g., for the transitions from the fully symmetric irrep).

[1] M. Göppert-Mayer, Ann. Phys. **401**, 273 (1931).
[2] W. Kaiser and C. G. B. Garrett, Phys. Rev. Lett. **7**, 229–231 (1961).
[3] W. R. Zipfel, R. M. Williams, and W. W. Webb, Nat. Biotechnol. **21**, 1369 (2003).
[4] F. Helmchen and W. Denk, Nat. Methods **2**, 932 (2005).
[5] K. Konig, J. Microsc. **200**, 83 (2000).
[6] A. Diaspro, G. Chirico, and M. Collini, Q. Rev. Biophys. **38**, 97 (2006).
[7] A. Hayat, A. Nevet, P. Ginzburg, and M. Orenstein, Semicond. Sci. Technol. **26**, 083001 (2011).
[8] M. Pawlicki, H. A. Collins, R. G. Denning, and H. L. Anderson, Angew. Chem., Int. Ed. **48**, 3244 (2009).
[9] B. Strehmel and V. Strehmel, "Owo-photon physical, organic, and polymer chemistry: Theory, techniques, chromophore design, and applications," in *Advances in Photochemistry*, edited by D. C. Neckers, W. S. Jenks, and T. Wolff (John Wiley & Sons, Inc., Hoboken, NJ, USA, 2007), Vol. 29, pp. 111–351.
[10] G. S. He, L.-S. Tan, Q. Zheng, and P. N. Prasad, Chem. Rev. **108**, 1245 (2008).
[11] H. M. Kim and B. R. Cho, Chem. Commun. **2009**, 153.
[12] C. Chung, D. Srikun, C. S. Lim, C. J. Chang, and B. R. Cho, Chem. Commun. **47**, 9618 (2011).
[13] S. Yao and K. D. Belfield, Eur. J. Org. Chem. **2012**, 3199.
[14] H. Yu, Y. Xiao, and L. Jin, J. Am. Chem. Soc. **134**, 17486 (2012).
[15] L. Li, J. Ge, H. Wu, Q.-H. Xu, and S. Q. Yao, J. Am. Chem. Soc. **134**, 12157 (2012).
[16] H.-Y. Ahn, K. E. Fairfull-Smith, B. J. Morrow, V. Lussini, B. Kim, M. V. Bondar, S. E. Bottle, and K. D. Belfield, J. Am. Chem. Soc. **134**, 4721 (2012).
[17] H. J. Kim, J. H. Han, M. K. Kim, C. S. Lim, H. M. Kim, and B. R. Cho, Angew. Chem., Int. Ed. **49**, 6786 (2010).
[18] T. Kowada, J. Kikuta, A. Kubo, M. Ishii, H. Maeda, S. Mizukami, and K. Kikuchi, J. Am. Chem. Soc. **133**, 17772 (2011).
[19] L. Yuan, W. Lin, H. Chen, S. Zhu, and L. He, Angew. Chem., Int. Ed. **52**, 10018–10022 (2013).
[20] F. Terenziani, C. Katan, E. Badaeva, S. Tretiak, and M. Blanchard-Desce, Adv. Mater. **20**, 4641 (2008).
[21] M. T. P. Beerepoot, D. H. Friese, and K. Ruud, Phys. Chem. Chem. Phys. **16**, 5958 (2014).
[22] W. M. McClain, J. Chem. Phys. **55**, 2789 (1971).
[23] W. M. McClain, Acc. Chem. Res. **7**, 129 (1974).
[24] R. L. Swofford and A. C. Albrecht, Annu. Rev. Phys. Chem. **29**, 421 (1978).
[25] C. G. Elles, C. Rivera, X. Zhang, P. A. Pieniazek, and S. E. Bradforth, J. Chem. Phys. **130**, 084501 (2009).
[26] D. A. Oulianov, I. V. Tomov, A. S. Dvornikov, and P. M. Rentzepis, Opt. Commun. **191**, 235–243 (2001).
[27] M. Drobizhev, N. S. Makarov, S. E. Tillo, T. E. Hughes, and A. Rebane, Nat. Methods **8**(5), 393 (2011).
[28] R. Nifosi and Y. Luo, J. Phys. Chem. B **111**, 505 (2007).
[29] M. G. Vivas, D. L. Silva, L. Misoguti, R. Zalesny, W. Bartkowiak, and C. R. Mendonca, J. Phys. Chem. A **114**, 3466 (2010).
[30] S. Tretiak and V. Chernyak, J. Chem. Phys. **119**, 8809 (2003).
[31] E. Kamarchik and A. I. Krylov, J. Phys. Chem. Lett. **2**, 488 (2011).
[32] A. H. Steindal, J. H. Olsen, K. Ruud, L. Frediani, and J. Kongsted, Phys. Chem. Chem. Phys. **14**, 5440 (2012).
[33] I. H. Nayyar, A. E. Masunov, and S. Tretiak, J. Phys. Chem. C **117**, 18170 (2013).
[34] M. J. Paterson, O. Christiansen, F. Pawowski, P. Jørgensen, C. Hättig, T. Helgaker, and P. Sałek, J. Chem. Phys. **124**, 054322 (2006).
[35] P. Salek, O. Vahtras, J. Guo, Y. Luo, T. Helgaker, and H. Argen, Chem. Phys. Lett. **374**, 446 (2003).
[36] O. Christiansen, H. Koch, and P. Jørgensen, Chem. Phys. Lett. **243**, 409 (1995).
[37] D. H. Friese, C. Hättig, and K. Ruud, Phys. Chem. Chem. Phys. **14**, 1175 (2012).
[38] M. A. Salem and A. Brown, J. Chem. Theory Comput. **10**, 3260 (2014).
[39] DALTON, a molecular electronic structure program, Release 2.0, 2005. See http://www.kjemi.uio.no/software/dalton/dalton.html.

[40]J. Olsen and P. Jørgensen, J. Chem. Phys. **82**, 3235 (1985).
[41]H. Koch and P. Jørgensen, J. Chem. Phys. **93**, 3333 (1990).
[42]TURBOMOLE v6.5 2013, a development of University of Karlsruhe and Forschungszentrum Karlsruhe GmbH, 1989-2007, TURBOMOLE GmbH, since 2007, http://www.turbomole.com.
[43]S. Knippenberg, D. R. Rehn, M. Wormit, J. H. Starcke, I. L. Rusakova, A. B. Trofimov, and A. Dreuw, J. Chem. Phys. **136**, 064107 (2012).
[44]Y. Shao, Z. Gan, E. Epifanovsky, A. T. B. Gilbert, M. Wormit, J. Kussmann, A. W. Lange, A. Behn, J. Deng, X. Feng, D. Ghosh, M. Goldey, P. R. Horn, L. D. Jacobson, I. Kaliman, R. Z. Khaliullin, T. Kus, A. Landau, J. Liu, E. I. Proynov, Y. M. Rhee, R. M. Richard, M. A. Rohrdanz, R. P. Steele, E. J. Sundstrom, H. L. Woodcock III, P. M. Zimmerman, D. Zuev, B. Albrecht, E. Alguires, B. Austin, G. J. O. Beran, Y. A. Bernard, E. Berquist, K. Brandhorst, K. B. Bravaya, S. T. Brown, D. Casanova, C.-M. Chang, Y. Chen, S. H. Chien, K. D. Closser, D. L. Crittenden, M. Diedenhofen, R. A. DiStasio, Jr., H. Do, A. D. Dutoi, R. G. Edgar, S. Fatehi, L. Fusti-Molnar, A. Ghysels, A. Golubeva-Zadorozhnaya, J. Gomes, M. W. D. Hanson-Heine, P. H. P. Harbach, A. W. Hauser, E. G. Hohenstein, Z. C. Holden, T.-C. Jagau, H. Ji, B. Kaduk, K. Khistyaev, J. Kim, J. Kim, R. A. King, P. Klunzinger, D. Kosenkov, T. Kowalczyk, C. M. Krauter, K. U. Laog, A. Laurent, K. V. Lawler, S. V. Levchenko, C. Y. Lin, F. Liu, E. Livshits, R. C. Lochan, A. Luenser, P. Manohar, S. F. Manzer, S.-P. Mao, N. Mardirossian, A. V. Marenich, S. A. Maurer, N. J. Mayhall, C. M. Oana, R. Olivares-Amaya, D. P. O'Neill, J. A. Parkhill, T. M. Perrine, R. Peverati, P. A. Pieniazek, A. Prociuk, D. R. Rehn, E. Rosta, N. J. Russ, N. Sergueev, S. M. Sharada, S. Sharmaa, D. W. Small, A. Sodt, T. Stein, D. Stuck, Y.-C. Su, A. J. W. Thom, T. Tsuchimochi, L. Vogt, O. Vydrov, T. Wang, M. A. Watson, J. Wenzel, A. White, C. F. Williams, V. Vanovschi, S. Yeganeh, S. R. Yost, Z.-Q. You, I. Y. Zhang, X. Zhang, Y. Zhou, B. R. Brooks, G. K. L. Chan, D. M. Chipman, C. J. Cramer, W. A. Goddard III, M. S. Gordon, W. J. Hehre, A. Klamt, H. F. Schaefer III, M. W. Schmidt, C. D. Sherrill, D. G. Truhlar, A. Warshel, X. Xu, A. Aspuru-Guzik, R. Baer, A. T. Bell, N. A. Besley, J.-D. Chai, A. Dreuw, B. D. Dunietz, T. R. Furlani, S. R. Gwaltney, C.-P. Hsu, Y. Jung, J. Kong, D. S. Lambrecht, W. Z. Liang, C. Ochsenfeld, V. A. Rassolov, L. V. Slipchenko, J. E. Subotnik, T. V. Voorhis, J. M. Herbert, A. I. Krylov, P. M. W. Gill, and M. Head-Gordon, Mol. Phys. **113**, 184 (2015).
[45]A. I. Krylov and P. M. W. Gill, WIREs Comput. Mol. Sci. **3**, 317 (2013).
[46]T. B. Pedersen and H. Koch, J. Chem. Phys. **106**, 8059 (1997).
[47]C. Hättig, O. Christiansen, and P. Jørgensen, J. Chem. Phys. **108**, 8331 (1998).
[48]C. Hättig, O. Christiansen, and P. Jørgensen, J. Chem. Phys. **108**, 8355 (1998).
[49]O. Christiansen, A. Halkier, H. Koch, P. Jørgensen, and T. Helgaker, J. Chem. Phys. **108**, 2801 (1998).
[50]C. Hättig and P. Jørgensen, J. Chem. Phys. **109**, 9219 (1998).
[51]O. Christiansen, P. Jørgensen, and C. Hättig, Int. J. Quantum Chem. **68**, 1 (1998).
[52]J. F. Stanton and R. J. Bartlett, J. Chem. Phys. **98**, 7029 (1993).
[53]R. J. Bartlett, Mol. Phys. **108**, 2905 (2010).
[54]N. H. F. Beebe and J. Linderberg, Int. J. Quantum Chem. **12**, 683 (1977).
[55]H. Koch, A. S. de Merás, and T. B. Pedersen, J. Chem. Phys. **118**, 9481 (2003).
[56]F. Aquilante, R. Lindh, and T. B. Pedersen, J. Chem. Phys. **127**, 114107 (2007).
[57]F. Aquilante, L. Gagliardi, T. B. Pedersen, and R. Lindh, J. Chem. Phys. **130**, 154107 (2009).
[58]F. Aquilante, T. B. Pedersen, and R. Lindh, Theor. Chem. Acc. **124**, 1 (2009).
[59]F. Aquilante, L. Boman, J. Boström, H. Koch, R. Lindh, A. S. de Merás, and T. B. Pedersen, "Cholesky decomposition techniques in electronic structure theory," *Linear-Scaling Techniques in Computational Chemistry and Physics*, Challenges and Advances in Computational Chemistry and Physics, edited by R. Zaleśny, M. G. Papadopoulos, P. G. Mezey, and J. Leszczynski (Springer, 2011), pp. 301–343.
[60]J. L. Whitten, J. Chem. Phys. **58**, 4496 (1973).
[61]M. W. Feyereisen, G. Fitzgerald, and A. Komornicki, Chem. Phys. Lett. **208**, 359 (1993).
[62]O. Vahtras, J. Almlöf, and M. W. Feyereisen, Chem. Phys. Lett. **213**, 514 (1993).
[63]A. Komornicki and G. Fitzgerald, J. Chem. Phys. **98**, 1398 (1993).
[64]D. E. Bernholdt and R. J. Harrison, Chem. Phys. Lett. **250**, 477 (1996).
[65]Y. Jung, A. Sodt, P. M. W. Gill, and M. Head-Gordon, Proc. Natl. Acad. Sci. U. S. A. **102**, 6692 (2005).
[66]F. Weigend, M. Kattannek, and R. Ahlrichs, J. Chem. Phys. **130**, 164106 (2009).
[67]F. Weigend, M. Häser, H. Patzelt, and R. Ahlrichs, Chem. Phys. Lett. **294**, 143 (1998).
[68]E. Epifanovsky, D. Zuev, X. Feng, K. Khistyaev, Y. Shao, and A. I. Krylov, J. Chem. Phys. **139**, 134105 (2013).
[69]A. Landau, K. Khistyaev, S. Dolgikh, and A. I. Krylov, J. Chem. Phys. **132**, 014109 (2010).
[70]R. J. Bartlett, Annu. Rev. Phys. Chem. **32**, 359 (1981).
[71]R. J. Bartlett and J. F. Stanton, Rev. Comput. Chem. **5**, 65 (1994).
[72]R. J. Bartlett, Int. J. Mol. Sci. **3**, 579 (2002).
[73]A. I. Krylov, Annu. Rev. Phys. Chem. **59**, 433 (2008).
[74]K. Sneskov and O. Christiansen, Wiley Interdiscip. Rev.: Comput. Mol. Sci. **2**, 566 (2012).
[75]R. J. Bartlett, Wiley Interdiscip. Rev.: Comput. Mol. Sci. **2**, 126 (2012).
[76]H. J. Monkhorst, Int. J. Quantum Chem. **12**, 421 (1977).
[77]D. Mukherjee and P. K. Mukherjee, Chem. Phys. **39**, 325 (1979).
[78]H. Sekino and R. J. Bartlett, Int. J. Quantum Chem. **26**, 255 (1984).
[79]H. Koch, H. J. Aa. Jensen, P. Jørgensen, and T. Helgaker, J. Chem. Phys. **93**, 3345 (1990).
[80]M. Head-Gordon and T. J. Lee, "Single reference coupled cluster and perturbation theories of electronic excitation energies," in *Modern Ideas in Coupled Cluster Theory*, edited by R. J. Bartlett (World Scientific, Singapore, 1997).
[81]The reference determines the separation of orbital space into the occupied and virtual subspaces. Here, we use indexes $i, j, k, \ldots$ and $a, b, c, \ldots$ to denote the orbitals from the two subspaces. To denote orbitals that can be either occupied or virtual, letters $p, q, r, s, \ldots$ will be used.
[82]S. V. Levchenko and A. I. Krylov, J. Chem. Phys. **120**, 175 (2004).
[83]R. M. Parrish, E. G. Hohenstein, T. J. Martínez, and C. D. Sherrill, J. Chem. Phys. **137**, 224106 (2012).
[84]E. G. Hohenstein, R. M. Parrish, C. D. Sherrill, and T. J. Martínez, J. Chem. Phys. **137**, 221101 (2012).
[85]L. D. Landau and E. M. Lifshitz, *Quantum Mechanics: Non-relativistic Theory* (Pergamon, Oxford, 1977).
[86]T. Helgaker, S. Coriani, P. Jørgensen, K. Kristensen, J. Olsen, and K. Ruud, Chem. Rev. **112**, 543 (2012).
[87]H. Koch, R. Kobayashi, A. S. de Merás, and P. Jørgensen, J. Chem. Phys. **100**, 4393 (1994).
[88]S. V. Levchenko, T. Wang, and A. I. Krylov, J. Chem. Phys. **122**, 224106 (2005).
[89]E. Epifanovsky, M. Wormit, T. Kuś, A. Landau, D. Zuev, K. Khistyaev, P. Manohar, I. Kaliman, A. Dreuw, and A. I. Krylov, J. Comput. Chem. **34**, 2293 (2013).
[90]See supplementary material at http://dx.doi.org/10.1063/1.4907715 for additional details.
[91]K. Kristensen, J. Kauczor, A. J. Thorvaldsen, P. Jorgensen, T. Kjaergaard, and A. Rizzo, J. Chem. Phys. **134**, 214104 (2011).
[92]K. Kristensen, J. Kauczor, T. Kjaergaard, and P. Jorgensen, J. Chem. Phys. **131**, 044112 (2009).
[93]D. E. Woon and T. H. Dunning, Jr., J. Chem. Phys. **100**, 2975 (1994).
[94]R. A. Kendall, Jr., T. H. Dunning, and R. J. Harrison, J. Chem. Phys. **96**, 6796 (1992).
[95]T. H. Dunning, J. Chem. Phys. **90**, 1007 (1989).
[96]F. Weigend, A. Köhn, and C. Hättig, J. Chem. Phys. **116**, 3175 (2002).
[97]H. Hosoi, S. Yarnaguchi, H. Mizuno, A. Miyawaki, and T. Tahara, J. Phys. Chem. B **112**, 2761 (2008).
[98]H. Kawano, T. Kogure, Y. Abe, H. Mizuno, and A. Miyawaki, Nat. Methods **5**, 373 (2008).
[99]A. D. Xia, S. Wada, H. Tashiro, and W. H. Huang, Arch. Bichem. Biophys. **372**, 280 (1999).
[100]M. Drobizhev, S. Tillo, N. S. Makarov, T. E. Hughes, and A. Rebane, J. Phys. Chem. B **113**, 855 (2009).
[101]R. Nifosi and Y. Luo, J. Phys. Chem. B **111**, 14043 (2007).
[102]It might be that the authors of Ref. 38 used excitation energy instead of the photon energy when computing macroscopic cross section using Eq. (32); this would lead to a factor of 4 difference in the cross section.